Sustained-release of Naproxen Sodium from Electrospun-aligned PLLA/PCL Scaffolds

Yuan Siang LUI[1,2,3], Mark P. LEWIS[2,3,4], Say Chye Joachim LOO[1,2,5*]

[1]School of Materials Science and Engineering
Nanyang Technological University
50 Nanyang Avenue Singapore 639798

[2]Institute for Sports Research
Nanyang Technological University
50 Nanyang Avenue Singapore 639798

[3]Loughborough University
School of Sport, Exercise and Health Sciences
Leicestershire, UK
LE11 3TU

[4]National Centre for Sport and Exercise Medicine England, Arthritis Research UK Centre for Sport, Exercise and Osteoarthritis, School of Sport, Exercise and Health Sciences, Loughborough University, UK

[5] Singapore Centre on Environmental Life Sciences Engineering (SCELSE), Nanyang Technological University, Singapore 637551

*Corresponding Author

Phone: +65-67904603

Fax: +65-67909081

Email: joachimloo@ntu.edu.sg

Abstract

Spontaneous tendon healing may result in reduced tissue functionality. In view of this, tissue engineering (TE) emerges as a promising approach in promoting proper tendon regeneration. However, unfavourable post-surgical adhesion formations restrict adequate tendon healing through the TE approach. Naproxen sodium (NPS), a non-steroidal anti-inflammatory drug (NSAID), has been demonstrated to prevent adhesions by inhibiting inflammatory response. Therefore, in this work, various factors, i.e. polymer composition (i.e. different poly-l-lactic acid (PLLA) to polycaprolactone (PCL) ratios) and percentage of water (H_2O) to hexafluoroisopropanol (HFIP) as co-solvent, were investigated to understand how these can influence the release of NPS from electrospun scaffolds. By adjusting the amount of H_2O as the co-solvent, NPS could be released sustainably for as long as two weeks. Scaffold breaking strength was also enhanced with the addition of H_2O as the co-solvent. This NPS-loaded scaffold showed no significant cytotoxicity, and L929 murine fibroblasts cultured on the scaffolds were able to proliferate and align along the fiber orientation. These scaffolds with desirable tendon TE characteristics would be promising candidates in achieving better tendon regeneration *in vivo*.

Keywords: Naproxen Sodium, Adhesion Formation, Electrospinning, PLLA, PCL, Tendon Regeneration

1 Introduction

According to statistics in the United States, 15 million musculoskeletal injuries involving the impairment of tendon and ligament are reported annually. Owing to the low cellularity and vascularity of these organs (Strauss et al., 2007), spontaneous healing commonly results in reduced tissue functionality (Sharma and Maffulli, 2006). In view of this, tissue engineering (TE) has emerged as a promising field that seeks to offer viable solutions to tissue regeneration, including tendon; whereby a three dimensional (3D) scaffold mimicking the cell microenvironment can be used to regenerate new tendon tissues. Key features of this scaffold include good biocompatibility, comparable degradation and tissue regeneration rates, and its degraded by-products must be safely eliminated through natural metabolic pathways (Rezwan et al., 2006; Salgado et al., 2004; Gunatillake and Adhikari, 2003; Vert et al., 1992). Since this scaffold would replace the tendon, it should also be able to withstand physical load and possess mechanical properties that matches with those of functional tissues (Sachlos and Czernuszka, 2003). This 3D structure would also require appropriate surface chemistry that permits cellular attachment and a porous structure allowing for tissue integration and diffusion of nutrients (Yang et al., 2001; Levenberg and Langer, 2004; Griffith, 2002). As such, tremendous research efforts have focused on mimicking the tendon microenvironment by using different materials as scaffold (Young et al., 1998; Funakoshi et al., 2005; Sahoo et al., 2006; Yin et al., 2010; Ladd et al., 2011), selecting appropriate cell types (Bi et al., 2007; Giovannini et al., 2008; Awad et al., 1999), and stimulating the regeneration of tendon cells either chemically (Wang, 2006; Chan et al., 2000; Wozney et al., 1988) or mechanically (Skutek et al., 2001; Sharma and Maffulli, 2005; Woo et al., 1981; Tanaka et al., 1995). Although the TE approach in facilitating tendon healing is

promising, the issue of post-surgical adhesion formation, which might eventually defer the success of tendon regeneration, is still inadequately addressed.

Adhesion formation, the result of overwhelming inflammatory response at the surgical site, refers to abnormal adherence of soft tissue to surrounding structures. Many factors, including surgical trauma, thermal injury, infection, foreign bodies and ischemia, could contribute to this undesirable fibrous ingrowth (Liakakos et al., 2001). Generally, during the tendon healing process, collagen will be secreted to restore the continuity of injured tendon fibrils. However, at the same time, there are large numbers of inflammatory cells being recruited to the injury site. Their unfavourable integration with fibrils between the tendon and sheath results in scar tissue formation that interferes with the gliding function of the tendon, eventually causing recurrent injury or loss of function (Sharma and Maffulli, 2006). Several attempts have been made to reduce these peritendious adhesions, including medical procedures involving modifications of surgical techniques (Zhao et al., 2001), tendon sheath closure (Strauch et al., 1985) and post-operative mobilization (Strickland and Glogovac, 1980; Wilson et al., 1990; Peck et al., 1998). However, there are some inconsistencies in the results reported from these. There are also studies that developed materials such as polyethylene tubes (Gonzalez, 1949), hydroxyapatite (Siddiqi et al., 1995) and silastic (Hunter and Salisbury, 1971) in a form of a pseudo-sheath to act as a barrier between the repaired tendon and surrounding tissues. Some studies have also indicated that the use of hyaluronic acid (Tanaka et al., 2007), which is a polysaccharide found in synovial fluid (Swann, 1978), could also decrease the overall quantity of tendon adhesions. However, there were still certain levels of adhesion tissue detected in the later stage of the experiments (Thomas et al., 1986).

One of the promising solutions in preventing adhesion formation is the prescription of NSAIDs, in particular Naproxen Sodium (NPS). NPS is a hydrophilic drug that is widely used as a pain reliever and also for the treatment of inflammation. It functions in a way of decreasing the metabolites and by-products of arachidonic acid by competitively inhibiting cyclo-oxygenase, thus reducing adhesion formation (Kulick et al., 1984; Akbulut et al., 2014). Therefore, it is desirable to develop a system that can release NPS locally and sustainably in order to minimize adhesion formation during tendon healing, while avoiding systemic over dosage which may lead to undesirable effects such as nausea, diarrhoea and abdominal pain (Berthold et al., 1996). So far, the employment of hydrophilic matrices or a direct compressing technique has been used to develop NPS-loaded products, as these methods are simple and cost-effective. However, drawbacks such as inadequate mechanical properties and a rapid release of NPS have limited its application in tissue engineering (Cifkova et al., 1990; BAE and Kim, 1993; Aher et al., 2014; Bhise et al., 2008). On the other hand, other attempts in releasing NPS from hydrophobic matrices (Bozdag et al., 2001; Bhoyar et al., 2011; Simonoska Crcarevska et al., 2008) were also not entirely successful, mainly due to the hydrophilicity and low molecular weight of NPS.

In view of these, this study attempts to address the above issues in tendon regeneration by developing a scaffold that possesses a combination of these desirable capabilities, i.e. sustained release of NPS, an aligned bio-mimicking environment, and possessing adequate mechanical properties. It is postulated that by manipulating electrospinning solution formulations, i.e. polymer ratios and co-solvent ratios, the distribution of NPS and thus its release can be

116 controlled. Hence, for the first time, hexafluro-2-propanol together with H_2O were used as
117 electrospinning solvents. It is therefore of interest to investigate how a cost-effective
118 electrospinning technique can be employed to develop drug-loaded, aligned fibers that can
119 potentially be used as a scaffold for tendon regeneration. These scaffolds fabricated through
120 different formulations were evaluated and characterized in terms of their morphology,
121 mechanical properties, *in-vitro* drug releasing ability and cell proliferation potential.

122

2 Materials and Methods

2.1 Fabrication of Electrospun Scaffolds

Poly-l-lactic acid (PLLA, intrinsic viscosity = 6.5 dl/g, Purac Biomaterials), Poly-caprolactone (PCL, Mw = 70,000 – 90,000, Sigma Aldrich), 1,1,1,3,3,3-hexafluoro-2-propanol (HFIP, Sigma Aldrich) and naproxen sodium (NPS, Sigma Aldrich) were used as received.

A total polymer concentration of 8 wt% PLLA/PCL blends (relative to solvent) was prepared. PLLA to PCL ratio was varied (i.e. 70:30, 80:20 and 90:10) to investigate effect of polymer compositions. 0.4 wt% NPS (relative to solvent) was dissolved directly together with PLLA/PCL blends and stirred overnight to ensure complete dissolution. In the subsequent *in vitro* drug release studies, mixtures of HFIP/H_2O were prepared by adding 3 %, 5 %, 7 % and 10 % (v/v) of deionized H_2O into HFIP. Scaffolds were named according to their PLLA ratio, followed by PCL ratio and its water volume percentage. For example, 70-30-0 indicated 70 wt% of PLLA blended with 30 wt% PCL, coupled with 0 % of H_2O in HFIP (shown in Table 1). Electrospinning was performed by using MECC Nanon-01A Electrospinning Setup. The solutions were dispensed from a single nozzle spinneret (22 gauge) at a constant feed rate of 1 ml/h and at accelerating voltage of 15 kV. Rotating speeds of 1500rpm were used in order to get fibers with aligned morphology. Fibers were collected by using a metallic mandrel set up fixed at 14 cm away from the tip of the spinneret.

2.2 Morphological Assessment of Electrospun Scaffolds

The morphologies of prepared scaffolds were analyzed by Field Emission Scanning Electron Microscopy (FESEM, JSM-6340F, JEOL Co.). The samples were platinum-coated at 20 mA for

60 s and imaged at an accelerating voltage of 5 kV. Mean fiber diameter was determined by measuring 50 independent fibers using Image J software (n=50).

2.3 *In Vitro* Drug Release Studies

Drug-loaded scaffolds were accurately weighed in triplicate, placed in vials containing 5mL of Phosphate Buffered Saline (PBS, pH = 7.4, OHME Scientific) and incubated at 37 °C in a shaking incubator. PBS was used because it possesses a physiologically relevant concentration of ions similar to the human body. At predetermined time intervals (1^{st}, 3^{rd}, 6^{th}, 9^{th} hour, 1 day, 2 days...), 1 mL of medium was removed from each vial and replenished with fresh PBS solution. Concentration of NPS was analyzed using a Shimadzu UV-2501 UV-Vis spectrophotometer (λ_{NPS} = 331 nm). The percentage cumulative release of the drug was studied as a function of incubation time (n=3).

2.4 Contact Angle and Water Uptake

Contact angle of the scaffolds was analyzed by using a static sessile drop technique on a contact angle goniometer. The measurements were conducted at room temperature in triplicate, with distilled H_2O being pumped out at a rate of 5 μL/s. The droplet was allowed to relax for 10 s before image was captured. Analysis was done with FTA32 software.

Three samples (1 cm X 1 cm) of each formulation were initially weighed (W_{dry}) prior to incubation in PBS maintained at 37 ºC. At predetermined time points, the films were washed with deionized

166 water and the excess blotted off before the wet weight (W_{wet}) was measured (n=3). The water uptake
167 was calculated according to the following equation:

$$Water\ Uptake\ (\%) = \frac{W_{wet} - W_{dry}}{W_{dry}} X\ 100\ \%$$

168

169 ## 2.5 Surface Properties of Electrospun Scaffolds

170 The presence and distribution of NPS within the electrospun fibers were determined by using X-
171 ray photon spectrometry (XPS). XPS was measured on a Kratos AXIS Ultra^{DLD} spectrometer
172 (Kratos Analytical Ltd.) with a mono Al Kα radiation source (hν = 1486.71 eV) operating at 5
173 mA and 15 kV (n=3).

174

175 ## 2.6 Mechanical Properties of Electrospun Scaffolds

176 The mechanical properties of the scaffolds were measured using Instron Tensile Machine 5567.
177 Samples were punched into standard dumbbell shape (according to ASTM D 638 – 08, type V
178 sample with thickness < 4 mm) and tested using a load cell of 500 N with a load generation of 5
179 mm min^{-1} at room temperature. Tensile strength (TS), strain at break (SB) and Young's modulus
180 (E) were calculated by measuring 3 samples for each formulation (n=3).

181

182 ## 2.7 Evaluation of Cell Viability and Morphology

183 *In vitro* cell culture studies were conducted by using L929 murine fibroblasts to assess the
184 biocompatibility of NPS-loaded aligned scaffolds. L929 were maintained in Dulbecco's

185 Modified Eagle Medium (DMEM) (PAA Laboratory) supplemented with 10 % Fetal Bovine
186 Serum (PAA Laboratory), 1 % L-Glutamine (200 mM, PAA Laboratory) and 1 % Penicillin-
187 Streptomycin (Gibco), at 37 ºC and 5 % CO_2.

188

189 Scaffolds were cut into circular discs of 2.15 cm diameter and UV-sterilized for 30 min and
190 rinsed three times with PBS. Cells were then seeded onto samples at a density of 5000 cells per
191 cm^2. The cell-seeded samples were incubated for 3 h at 37 ºC and 5 % CO2 to allow cell
192 attachment. Tissue culture polystyrene (TCPS) was used as the control. Subsequently, each well
193 was filled with 1 ml of complete DMEM. Medium was changed every 3 days.

194

195 Cell viability was evaluated in triplicate using the Live/Dead staining assay (n=3). At
196 predetermined time intervals (day 1, day 3 and day 7), cell cultured samples were rinsed once
197 with PBS and incubated in a mixture of 2 μM Calcein-AM (Invitrogen) and 4 μM ethidium
198 homodimer-1 (Invitrogen) in PBS at 37 ºC for 15 min. Samples were subsequently rinsed once
199 again in PBS and transferred onto the glass coverslips for imaging under a fluorescence (Nikon
200 80i) using a 10x objective lens. Images were analysed by using Image J 1.44f software.

201

202 **2.8 Statistical Analysis**

203 All data were expressed as mean ± standard deviation (SD). Comparisons between groups were
204 made with one way ANOVA followed by Tukey's HSD post hoc test on SPSS version 11.5.
205 Differences were considered statistically significant at value of $p < 0.05$.

206

3 Results

3.1 Morphological Assessment

FESEM analysis was done to evaluate the microstructure of scaffolds. Figure 1 shows that all formulations with NPS were successfully electrospun into well-aligned fibers with beadless morphology. It was found that increasing the PCL to PLLA ratio had no significant effect on fiber diameter (70-30-0: 0.944 ± 0.096 μm; 80-20-0: 1.090 ± 0.233 μm; 90-10-0: 1.071 ± 0.153 μm), as shown in Figure 2A, and all fibers had approximately similar mean diameters of ~1μm.

With the introduction of H_2O as the co-solvent, fiber diameter was observed to decrease, as shown in Figure 2B. Mean fiber diameter decreased from 1.071 ± 0.153 μm to 0.760 ± 0.176 μm, when H_2O was added up to 10 % ($p < 0.001$).

3.2 In Vitro Drug Release Studies

Figure 3A shows the *in vitro* drug release profiles of the scaffolds for different PCL to PLLA ratios. NPS released rapidly from 90-10-0, 80-20-0 and 70-30-0, with first hour release recorded at 24.11 ± 1.45 %, 55.05 ± 0.23 % and 66.28 ± 2.05 % of the total drug loaded respectively. 80-20-0 and 70-30-0 could release NPS for only a day, whereas 90-10-0 was able to release NPS for up to three days. These samples were without H_2O as co-solvent.

The effect of co-solvent (i.e. H_2O) on NPS release was shown in Figure 3B. At 3 vol% of H_2O, NPS release rate was significantly reduced. Release was also found to be sustained for up to two

227 weeks with a relatively low burst release (2.79 ± 0.76 %) within the first hour. Similarly, low
228 burst release was observed for 90-10-5, 90-10-7, 90-10-10, but their subsequent release rates
229 were faster than 90-10-3. 90-10-5 could sustain the release of NPS for up to ten days, but release
230 was less than seven days for 90-10-7 and 90-10-10. It should be noted that the spectra obtained
231 were similar to the spectrum of the first day, indicating that there was no deterioration of the
232 NPS bioactivity throughout the experiment.

233

234 ## 3.3 Contact Angle and Water Uptake

235 Contact angle and water uptake measurements were conducted to evaluate the hydrophilicities of
236 the scaffolds which would influence the associated release profiles. Figure 4 shows the contact
237 angles of various scaffolds in which the electrospinning solutions were prepared in different
238 formulations. Figure 4A shows that the contact angle of 90-10-0 scaffold was significantly
239 higher than that of 80-20-0 and 70-30-0. The introduction of H_2O as co-solvent from 3 vol%, to
240 10 vol% gave no significant change in the contact angle (as shown in Figure 4B).

241

242 Figure 5 shows the water uptake of various scaffolds, in which the electrospinning solutions
243 were prepared in different formulations, after 7 days of immersion in PBS. Generally, 70-30-0
244 and 80-20-0 scaffolds have a significantly higher water uptake than that of the 90-10-0 as shown
245 in Figure 5A. Meanwhile the addition of H_2O as co-solvent did not significantly change the
246 water uptake of the scaffolds (Figure 5B).

247

3.4 X-ray Photon Spectrometry

Figure 6 shows the XPS analysis of scaffolds with and without NPS. The presence of NPS on scaffold 90-10-0, 90-10-3 and 90-10-10 was indicated by the sodium characteristic peak (Na 4s), which was at the binding energy of around 1071 eV, while 90-10 (No NPS) showed no peak at that particular region. The area under the spectra corresponds to the amount of NPS present on the surface of the fibers (depth of 0-10nm). Higher amount of NPS was detected when no water was added as the co-solvent (90-10-0, Figure 6), while relatively lower NPS amount was detected on 90-10-3 scaffolds (Figure 6). However, further increasing the amount of co-solvent to 10 vol% yielded a spectrum with an intermediate area that was laid between 90-10-0 and 90-10-3.

3.5 Mechanical Testing

Figure 7 and Table 2 show the mechanical properties of various fibrous scaffolds. When considering the effect of polymer compositions, the increase of PCL to PLLA ratio did not significantly alter the Young's modulus (E, Figure 7A) and tensile strength (TS, Table 2) of the scaffolds, which were of average 300 MPa and 25 MPa respectively. However, the increase of PCL to PLLA ratio improved the elasticity of the scaffolds, as shown in Figure 6A. The strain at break (SB) improved as more PCL was added: 90-10-0 < 80-20-0 ~ 70-30-0.

Figure 7B plots the E and TS of the various scaffolds when changing the H_2O percentage as co-solvent. It shows that the addition of the H_2O did not significantly alter the E and TS of the

scaffolds, which were on average 250 MPa and 15 MPa respectively. However, from Figure 7B, 90-10-3 scaffold has yielded the maximum SB value, which was at 51.29 ± 5.56 %. This is significantly higher than the other samples which yielded lower SB value. It is worth mentioning that all the formulations have yielded scaffolds with similar values in comparison with tendon, fracturing at about 8-10% (Sharma and Maffulli, 2006). Higher strain to break values gives materials better ability to withstand long term loading, which is essentially important especially for tendon TE.

3.6 *In Vitro* Cell Viability Studies

Preliminary cell viability study has been carried out to evaluate the cytotoxicity of the optimized scaffolds. L929 murine fibroblasts viability on the NPS-loaded scaffold (90-10-3) was evaluated using the Live/Dead staining assay. Fluorescence images of L929 cultured samples are shown in Figure 8. On day 1 of culture, viable cells were evident on both NPS-loaded scaffolds as well as TCPS, which was the positive control in the study. On day 3, it was notable that a small proportion of cells started to spread into their typical spindle morphology on NPS loaded scaffolds while some cells on TCPS adopted highly spread morphology. By day 7, cells on random NPS loaded scaffolds and TCPS were quite confluent but some were rounded. In contrast, cells on the aligned NPS-loaded scaffolds exhibited a high degree of spreading and arranged themselves according to the alignment of the scaffolds.

4 Discussion

In order to achieve tendon regeneration through TE, it is important to consider not just a biocompatible and mechanically sound scaffold that allows for good cell attachment and proliferation, but also one that can avoid undesirable adhesion formations during tendon healing. As such, the approach in this study is to achieve a sustained release of NPS from a biodegradable scaffold that can minimize any adhesion formation (Cifkova et al., 1990; BAE and Kim, 1993). With this, several parameters were investigated, including polymer formulation, and the use of H2O as a co-solvent with HFIP.

The scaffold was fabricated by using electrospinning as a technique to mimic the extracellular matrix (ECM) of a tendon. The tendon ECM consists of well-aligned, closely-packed collagen fiber; hence, the need for an aligned fiber morphology in order to mimic this micro-environment. For instance, Yin et al. demonstrated the tendency of tendon genesis of human tendon stem/progenitor cells (hTSPCs) only when they were cultured on aligned nanofibers rather than random nanofibers. A well-aligned morphology is therefore deemed as an essential criterion. By using a rotating mandrel setup, NPS-loaded PLLA/PCL scaffolds with aligned morphology were successfully prepared. It was also noted that a higher mandrel speed (1500 rpm) would result in better fiber alignment (Matthews et al., 2002). Other than fiber orientation, fiber diameter was also an important consideration in tendon TE because it has been shown that fiber diameter affects the regulation of tendon cell responses. Increasing the PCL to PLLA ratio was found to have no effect on fiber diameter. However, fiber diameter decreased with increasing co-solvent

312 (i.e. H_2O) percentage. This could be because of a lower actual mass of polymer solution being
313 ejected out at the tip of the spinneret due to larger proportion of H_2O (Xie and Buschle‐Diller,
314 2010). Another reason could be that the addition of H_2O into HFIP increased the dielectric
315 constant of HFIP/H_2O solutions, resulting in fibers that are more highly stretched during
316 electrospinning, and hence thinner fibers (Fioroni et al., 2001; Meechaisue et al., 2006). Overall,
317 the resultant fiber diameter from all formulations in this study was in the submicron range. This
318 highlights the potential of these scaffolds for tendon TE as the submicron ranged fibers (0.3μm-
319 0.7μm) were shown to promote cell proliferation and production of collagen and proteoglycans
320 which are essential for tendon healing (Erisken et al., 2012).

321

322 Despite the successful fabrication of scaffolds with the desired morphological properties for
323 tendon TE, the major issue still lies in the ability to control the release of NPS in preventing
324 adhesion formations. To address this, several attempts, such as the loading of NPS into PLGA
325 microspheres, lipid-like carnauba wax microparticles, Eudragit S-100 coated sodium alginate
326 microspheres and electrospun cellulose acetate scaffolds, had been reported (Bozdag et al., 2001;
327 Bhoyar et al., 2011; Simonoska Crcarevska et al., 2008). However, so far, these systems were
328 only able to achieve short NPS release profiles from a few hours to a few days due to the very
329 hydrophilic nature and low molecular weight of NPS. Certainly, such short release profile would
330 be insufficient to achieve any good function, since inflammation may last for as long as two
331 weeks. Various formulations, such as polymer compositions and H_2O percentage in HFIP, were
332 therefore investigated for their ability to tune drug release rates.

333

334 It was found that higher PCL to PLLA ratio of the fibers would lead to a further increase in NPS
335 release rate. This is because at 37ºC (the release condition), PCL chains are in a highly mobile
336 and flexible rubbery state with sufficient free volume due to its low Tg (~-60ºC) (Chen et al.,
337 2010; Lao et al., 2008). With more PCL, scaffolds exhibited higher wettability and water uptake
338 (Figure 4A and Figure 5A). This increases the solubility of hydrophilic NPS and promotes its
339 diffusion towards the fiber surface, resulting in a relatively faster release. On the contrary, it was
340 found that when H_2O was introduced at 3 vol% as a co-solvent, it led to a desirable slow release
341 of NPS. It is postulated that the presence of H_2O as co-solvent could have led to the formation of
342 two different phases within the fiber, caused by a change in the evaporation rate of the final
343 solvent. During electrospinning, HFIP evaporates faster than H_2O, and this might have resulted
344 in the formation of polymer shells trapping the H_2O phase within the fiber. NPS, being
345 hydrophilic, prefers to remain in the H_2O phase and resides inside the fiber with the H_2O phase
346 (Figure 9). XPS analysis in Figure 6 shows that there was also lower amount of NPS on the fiber
347 surface when 3 vol% of H_2O was introduced, hence indicating that more NPS resided in the core
348 of the fiber (Figure 9). However, this effect would be countered when the content of H_2O in the
349 electrospinning solution increased further beyond 3 vol%. With increasing H_2O content, thinner
350 fiber would be produced due to more fiber stretching. Thinner fibers would have a higher surface
351 area to volume ratio, thus facilitating a higher release rate (Chen et al., 2012). In addition, XPS
352 analysis indicated that further increasing H_2O content to 10 vol% resulted in having more NPS
353 on the fiber surface. Therefore, the release rate of NPS is dependent on a balance between
354 evaporation rate and fiber thickness. Overall, a desirable NPS release profile was achieved for up
355 to two weeks when PLLA to PCL ratio was 90:10 with 3 vol% of H_2O added as co-solvent – a

356 sustained release period that has never been reported in the literature, due to the challenge
357 involved in controlling the release of a hydrophilic drug such as NPS.

358

359 Given the NPS release results, scaffold electrospun with the 90-10-3 formulation was further
360 evaluated for its potential as a TE scaffold for tendon regeneration. A natural tendon exhibits a
361 very high Young's modulus of about 1.2-1.6 GPa (Bennett et al., 1986). In order to match the
362 Young's modulus of a tendon, PLLA was considered as the candidate polymer in this work due
363 to its high modulus and biocompatibility. However, PLLA is brittle and hence PCL was
364 introduced into the formulations to improve elasticity, since the presence of PCL can disrupt the
365 crystallinity of PLLA resulting in improved elongation (Wong et al., 2008). All formulations
366 could be electrospun into scaffolds with relatively strong mechanical properties ranging from
367 250 to 300 MPa and 15 to 25 MPa for their Young's modulus (E) and tensile strength (TS)
368 respectively. Although there are no significant differences in E and TS among these scaffolds
369 from different formulations, significant differences in elasticity could be observed when
370 formulations varied in their composition of the co-solvent (i.e. H_2O). In this study, evaluating the
371 effect of H_2O on the mechanical properties was only done on scaffolds electrospun from
372 formulations with 90:10 PLLA/PCL composition because this had the most desirable NPS
373 release profile. It was found that the formulation of the scaffold with the highest elasticity was
374 achieved when 3 vol% H_2O was used, while a formulation with no H_2O content and formulations
375 with H_2O content higher than 3 vol% produced scaffolds with significantly lower elasticity. A
376 solvent mixture with a higher boiling point would lead to a higher degree of molecular
377 orientation of the polymer chains within the fiber (as shown in Figure 10), and hence an
378 enhancement of elasticity (Wong et al., 2008; Asran et al., 2010). However, further increasing

H_2O percentage resulted in highly stretched polymer chains within the fiber and hence lower elasticity of the scaffolds was observed (Tan et al., 2005). Overall, it was worthy to note that scaffold electrospun out of the formulation of 90-10-3 not only possess the highest elasticity but also the most desirable NPS release profile.

These scaffolds were also evaluated for their biocompatibility and ability to induce cell response. Immortalized L929 murine fibroblasts were used as recommended by ASTM (ASTM F813-07: Standard Practice for Direct Contact Cell Culture Evaluation of Materials for Medical Devices). From Live/Dead staining, it can be seen that the NPS-loaded scaffolds were found to be non-cytotoxic and were able to induce healthy cellular response and proliferation. L929 cells were able to arrange themselves according to the fibers alignment on day 7 of culture. This observation is essential in tendon TE as cells that are able to adopt the aligned morphology of the scaffolds would have higher tendency in tendon genesis (Yin et al., 2010).

5 Conclusion

In this work, the feasibility to load NPS into electrospun PLLA/PCL scaffolds with aligned, beadless and continuous fibrous morphology was demonstrated. Different formulations of electrospinning solutions were investigated for their effect on NPS release. Increasing PCL content resulted in a higher strain at break, but a faster release rate of NPS. By adjusting the H_2O percentage with HFIP, a two-week sustained release could be achieved in a scaffold with optimal mechanical properties. *In vitro* cell studies showed that L929 cells could proliferate and align to the fiber orientation. These optimized PLLA/PCL scaffolds possess both sustained NPS releasing

ability and desirable tendon TE characteristics, and could have good potential in achieving better tendon regeneration.

6. Acknowledgements

The authors would like to thank Assistant Professor Leong Tai Wei David and Ms Magdiel Inggrid Setyawati from National University of Singapore for their kind assistance in XPS analysis. The authors would also like to acknowledge the financial support from the Institute for Sports Research, the Singapore Centre on Environmental Life Sciences Engineering (SCELSE) (M4330001.C70.703012), the School of Materials Science and Engineering (M020070110), National Medical Research Council, Ministry of Health (NMRC/CIRG/1342/2012, MOH), and the NTU-National Healthcare Group (NTU-NHG) grant (ARG/14012). This study was supported financially by the Arthritis Research UK Centre for Sport, Exercise and Osteoarthritis (Grant reference 20194) and this research was supported by the National Centre for Sport and Exercise Medicine (NCSEM) England, a collaboration between several sporting bodies, public bodies, universities and NHS Trusts nationally. The views expressed are those of the authors and not necessarily those of the NCSEM England or the partners involved.

References

Aher SJ, Jagdale S and Dhachinamoorthi D. (2014) Formulation and evaluation of colon specific drug delivery of naproxen sodium using guar gum and xanthan gum. *Indo American Journal of Pharmaceutical Research* 4: 1530-1538.

Akbulut N, Üstüner E, Atakan C, et al. (2014) Comparison of the effect of naproxen, etodolac and diclofenac on postoperative sequels following third molar surgery: A randomised, double-blind, crossover study. *Medicina oral, patologia oral y cirugia bucal* 19: e149.

Asran AS, Salama M, Popescu C, et al. (2010) Solvent Influences the Morphology and Mechanical Properties of Electrospun Poly(L-lactic acid) Scaffold for Tissue Engineering Applications. *Macromolecular Symposia* 294: 153-161.

Awad HA, Butler DL, Boivin GP, et al. (1999) Autologous mesenchymal stem cell-mediated repair of tendon. *Tissue engineering* 5: 267-277.

BAE Y and Kim SW. (1993) Hydrogel delivery systems based on polymer blends, block co-polymers or interpenetrating networks. *Advanced drug delivery reviews* 11: 109-135.

Bennett M, Ker R, Imery NJ, et al. (1986) Mechanical properties of various mammalian tendons. *Journal of Zoology* 209: 537-548.

Berthold A, Cremer K and Kreuter J. (1996) Preparation and characterization of chitosan microspheres as drug carrier for prednisolone sodium phosphate as model for anti-inflammatory drugs. *Journal of Controlled Release* 39: 17-25.

Bhise KS, Dhumal RS, Paradkar AR, et al. (2008) Effect of drying methods on swelling, erosion and drug release from chitosan–naproxen sodium complexes. *AAPS PharmSciTech* 9: 1-12.

Bhoyar P, Morani D, Biyani D, et al. (2011) Encapsulation of naproxen in lipid-based matrix microspheres: Characterization and release kinetics. *Journal of young pharmacists: JYP* 3: 105.

Bi Y, Ehirchiou D, Kilts TM, et al. (2007) Identification of tendon stem/progenitor cells and the role of the extracellular matrix in their niche. *Nature medicine* 13: 1219-1227.

Bozdag S, Calis S, Kas H, et al. (2001) In vitro evaluation and intra-articular administration of biodegradable microspheres containing naproxen sodium. *Journal of microencapsulation* 18: 443-456.

Chan BP, Fu S-c, Qin L, et al. (2000) Effects of basic fibroblast growth factor (bFGF) on early stages of tendon healing: a rat patellar tendon model. *Acta Orthopaedica* 71: 513-518.

Chen L, Yang J, Wang K, et al. (2010) Largely improved tensile extensibility of poly (L‐lactic acid) by adding poly (ε‐caprolactone). *Polymer International* 59: 1154-1161.

Chen S, Huang X, Cai X, et al. (2012) The influence of fiber diameter of electrospun poly (lactic acid) on drug delivery. *Fibers and Polymers* 13: 1120-1125.

Cifkova I, Lopour P, Vondráček P, et al. (1990) Silicone rubber-hydrogel composites as polymeric biomaterials: I. Biogical properties of the silicone rubber-p (HEMA) composite. *Biomaterials* 11: 393-396.

Erisken C, Zhang X, Moffat KL, et al. (2012) Scaffold fiber diameter regulates human tendon fibroblast growth and differentiation. *Tissue Engineering Part A* 19: 519-528.

Fioroni M, Burger K, Mark AE, et al. (2001) Model of 1, 1, 1, 3, 3, 3-hexafluoro-propan-2-ol for molecular dynamics simulations. *The Journal of Physical Chemistry B* 105: 10967-10975.

Funakoshi T, Majima T, Iwasaki N, et al. (2005) Application of tissue engineering techniques for rotator cuff regeneration using a chitosan-based hyaluronan hybrid fiber scaffold. *The American journal of sports medicine* 33: 1193-1201.

Giovannini S, Brehm W, Mainil‐Varlet P, et al. (2008) Multilineage differentiation potential of equine blood‐derived fibroblast‐like cells. *Differentiation* 76: 118-129.
Gonzalez RI. (1949) Experimental tendon repair within the flexor tunnels: use of polyethylene tubes for improvement of functional results in the dog. *Surgery* 26: 11.
Griffith LG. (2002) Emerging design principles in biomaterials and scaffolds for tissue engineering. *Annals of the New York Academy of Sciences* 961: 83-95.
Gunatillake PA and Adhikari R. (2003) Biodegradable synthetic polymers for tissue engineering. *Eur Cell Mater* 5: 1-16.
Hunter JM and Salisbury RE. (1971) Flexor-Tendon Reconstruction in Severely Damaged Hands A TWO-STAGE PROCEDURE USING A SILICONE-DACRON REINFORCED GLIDING PROSTHESIS PRIOR TO TENDON GRAFTING. *The Journal of Bone & Joint Surgery* 53: 829-858.
Kulick MI, Brazlow R, Smith S, et al. (1984) Injectable ibuprofen: preliminary evaluation of its ability to decrease peritendinous adhesions. *Annals of plastic surgery* 13: 459-467.
Ladd MR, Lee SJ, Stitzel JD, et al. (2011) Co-electrospun dual scaffolding system with potential for muscle–tendon junction tissue engineering. *Biomaterials* 32: 1549-1559.
Lao LL, Venkatraman SS and Peppas NA. (2008) Modeling of drug release from biodegradable polymer blends. *European Journal of Pharmaceutics and Biopharmaceutics* 70: 796-803.
Levenberg S and Langer R. (2004) Advances in tissue engineering. *Current topics in developmental biology* 61: 113-134.
Liakakos T, Thomakos N, Fine PM, et al. (2001) Peritoneal adhesions: etiology, pathophysiology, and clinical significance. *Digestive surgery* 18: 260-273.
Matthews JA, Wnek GE, Simpson DG, et al. (2002) Electrospinning of collagen nanofibers. *Biomacromolecules* 3: 232-238.
Meechaisue C, Dubin R, Supaphol P, et al. (2006) Electrospun mat of tyrosine-derived polycarbonate fibers for potential use as tissue scaffolding material. *Journal of Biomaterials Science, Polymer Edition* 17: 1039-1056.
Peck F, Bücher C, Watson J, et al. (1998) A comparative study of two methods of controlled mobilization of flexor tendon repairs in zone 2. *The Journal of Hand Surgery: British & European Volume* 23: 41-45.
Rezwan K, Chen Q, Blaker J, et al. (2006) Biodegradable and bioactive porous polymer/inorganic composite scaffolds for bone tissue engineering. *Biomaterials* 27: 3413-3431.
Sachlos E and Czernuszka J. (2003) Making tissue engineering scaffolds work. Review: the application of solid freeform fabrication technology to the production of tissue engineering scaffolds. *Eur Cell Mater* 5: 39-40.
Sahoo S, Ouyang H, Goh JC-H, et al. (2006) Characterization of a novel polymeric scaffold for potential application in tendon/ligament tissue engineering. *Tissue engineering* 12: 91-99.
Salgado AJ, Coutinho OP and Reis RL. (2004) Bone tissue engineering: state of the art and future trends. *Macromolecular bioscience* 4: 743-765.
Sharma P and Maffulli N. (2005) Tendon injury and tendinopathy: healing and repair. *The Journal of Bone & Joint Surgery* 87: 187-202.
Sharma P and Maffulli N. (2006) Biology of tendon injury: healing, modeling and remodeling. *Journal of Musculoskeletal and Neuronal Interactions* 6: 181.
Siddiqi NA, Hamada Y, Ide T, et al. (1995) Effects of hydroxyapatite and alumina sheaths on postoperative peritendinous adhesions in chickens. *Journal of Applied Biomaterials* 6: 43-53.
Simonoska Crcarevska M, Glavas Dodov M and Goracinova K. (2008) Chitosan coated Ca–alginate microparticles loaded with budesonide for delivery to the inflamed colonic mucosa. *European Journal of Pharmaceutics and Biopharmaceutics* 68: 565-578.

Skutek M, Griensven M, Zeichen J, et al. (2001) Cyclic mechanical stretching modulates secretion pattern of growth factors in human tendon fibroblasts. *European journal of applied physiology* 86: 48-52.
Strauch B, De Moura W, Ferder M, et al. (1985) The fate of tendon healing after restoration of the integrity of the tendon sheath with autogenous vein grafts. *The Journal of hand surgery* 10: 790-795.
Strauss EJ, Ishak C, Jazrawi L, et al. (2007) Operative treatment of acute Achilles tendon ruptures: an institutional review of clinical outcomes. *Injury* 38: 832-838.
Strickland JW and Glogovac S. (1980) Digital function following flexor tendon repair in zone II: a comparison of immobilization and controlled passive motion techniques. *The Journal of hand surgery* 5: 537-543.
Swann D. (1978) Macromolecules of synovial fluid. *The joints and synovial fluid* 1: 407-435.
Tan E, Ng S and Lim C. (2005) Tensile testing of a single ultrafine polymeric fiber. *Biomaterials* 26: 1453-1456.
Tanaka H, Manske PR, Pruitt DL, et al. (1995) Effect of cyclic tension on lacerated flexor tendons< i> in vitro</i>. *The Journal of hand surgery* 20: 467-473.
Tanaka T, Zhao C, Sun Y-L, et al. (2007) The Effect of Carbodiimide-Derivatized Hyaluronic Acid and Gelatin Surface Modification on Peroneus Longus Tendon Graft in a Short-Term Canine Model< i> In Vivo</i>. *The Journal of hand surgery* 32: 876-881.
Thomas S, Jones L and Hungerford D. (1986) Hyaluronic acid and its effect on postoperative adhesions in the rabbit flexor tendon: a preliminary look. *Clinical orthopaedics and related research* 206: 281-289.
Vert M, Li S, Spenlehauer G, et al. (1992) Bioresorbability and biocompatibility of aliphatic polyesters. *Journal of materials science: Materials in medicine* 3: 432-446.
Wang JH-C. (2006) Mechanobiology of tendon. *Journal of biomechanics* 39: 1563-1582.
Wilson K, Moore M, Rayner C, et al. (1990) Extensor tendon repair: an animal model which allows immediate post-operative mobilisation. *The Journal of Hand Surgery: British & European Volume* 15: 74-78.
Wong S-C, Baji A and Leng S. (2008) Effect of fiber diameter on tensile properties of electrospun poly (ε-caprolactone). *Polymer* 49: 4713-4722.
Woo S, Gomez M, Woo Y, et al. (1981) Mechanical properties of tendons and ligaments. II. The relationships of immobilization and exercise on tissue remodeling. *Biorheology* 19: 397-408.
Wozney JM, Rosen V, Celeste AJ, et al. (1988) Novel regulators of bone formation: molecular clones and activities. *Science* 242: 1528-1534.
Xie Z and Buschle‐Diller G. (2010) Electrospun poly (D, L‐lactide) fibers for drug delivery: The influence of cosolvent and the mechanism of drug release. *Journal of Applied Polymer Science* 115: 1-8.
Yang S, Leong K-F, Du Z, et al. (2001) The design of scaffolds for use in tissue engineering. Part I. Traditional factors. *Tissue engineering* 7: 679-689.
Yin Z, Chen X, Chen JL, et al. (2010) The regulation of tendon stem cell differentiation by the alignment of nanofibers. *Biomaterials* 31: 2163-2175.
Young RG, Butler DL, Weber W, et al. (1998) Use of mesenchymal stem cells in a collagen matrix for Achilles tendon repair. *Journal of orthopaedic research* 16: 406-413.
Zhao C, Amadio PC, Momose T, et al. (2001) The effect of suture technique on adhesion formation after flexor tendon repair for partial lacerations in a canine model. *The Journal of Trauma and Acute Care Surgery* 51: 917-921.

Figure Captions

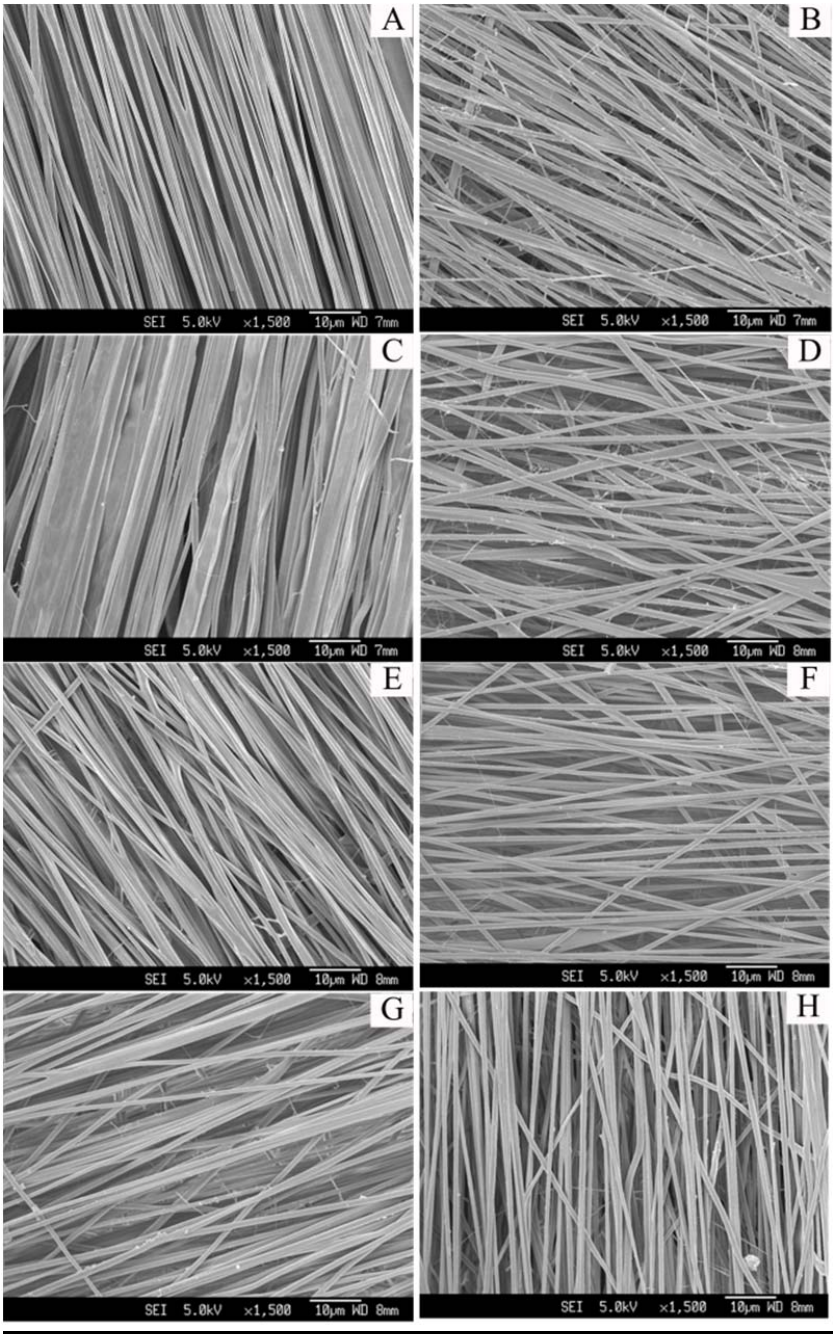

Figure 1: (A) Formulation without NPS was optimized in order to obtain aligned morphology. Using the same parameters, different formulations of electrospinning solutions with fixed amount of NPS, (B) 70-30-0; (C) 80-20-0; (D) 90-10-0; (E) 90-10-3; (F) 90-10-5; (G) 90-10-7; (H) 90-10-10, were successfully electrospun into aligned fibers with beadless morphology. (Scale bar = 10μm).

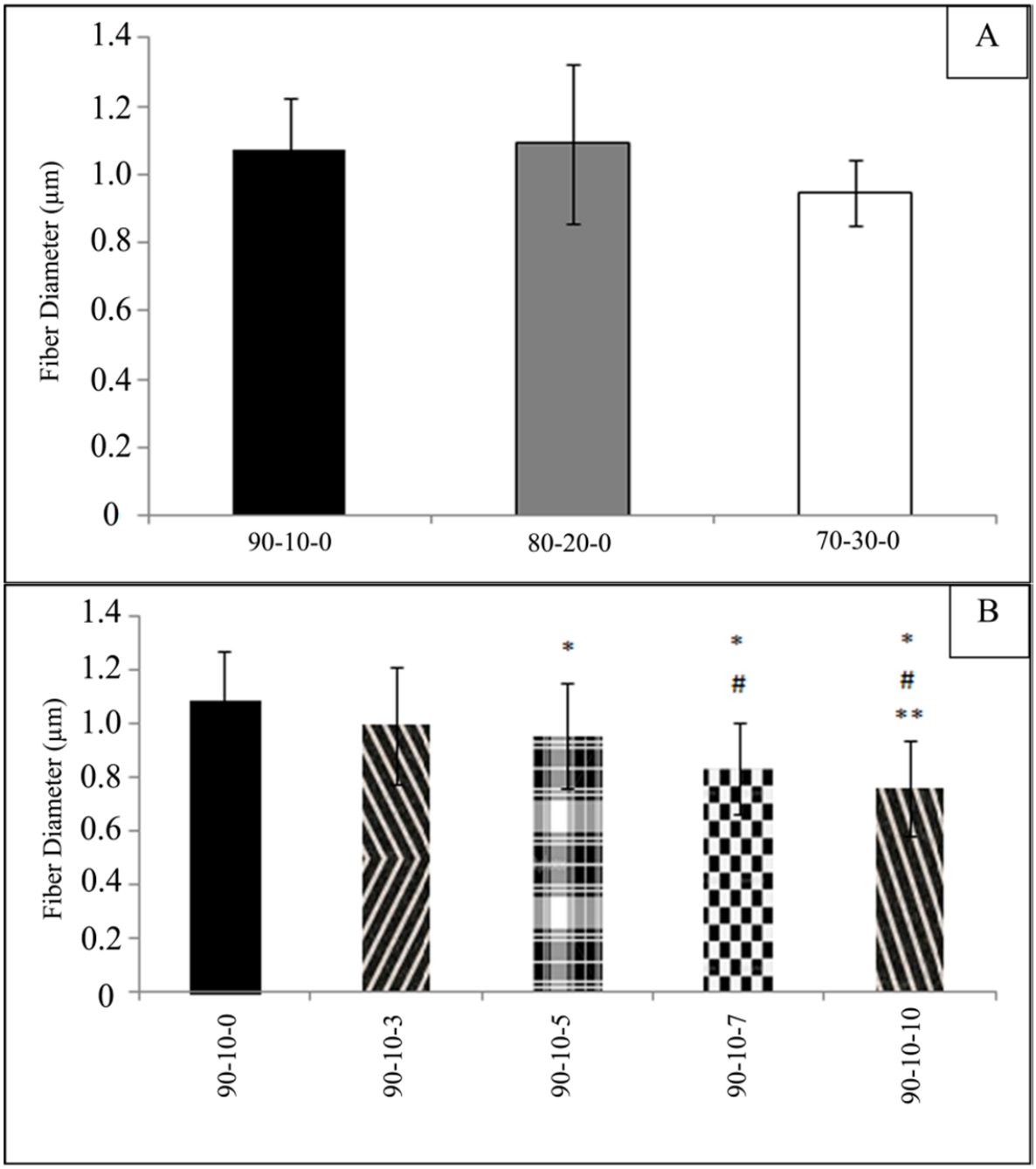

563

564 **Figure 2:** Comparison of fibers diameter when the (A) polymer composition, i.e. PCL to PLLA ratio, and
565 (B) co-solvent composition, i.e. H_2O to HFIP ratio, were varied. There was no significant difference in
566 fibers diameter when changing the PCL content. A decreasing trend in fibers diameter was observed when
567 the H_2O percentage was increased *(* indicates $p < 0.05$ with respect to 90-10-0; # indicates $p < 0.05$ with*
568 *respect to 90-10-3; ** indicates $p < 0.05$ with respect to 90-10-5).* (Error bars indicate standard deviation,
569 n = 50).

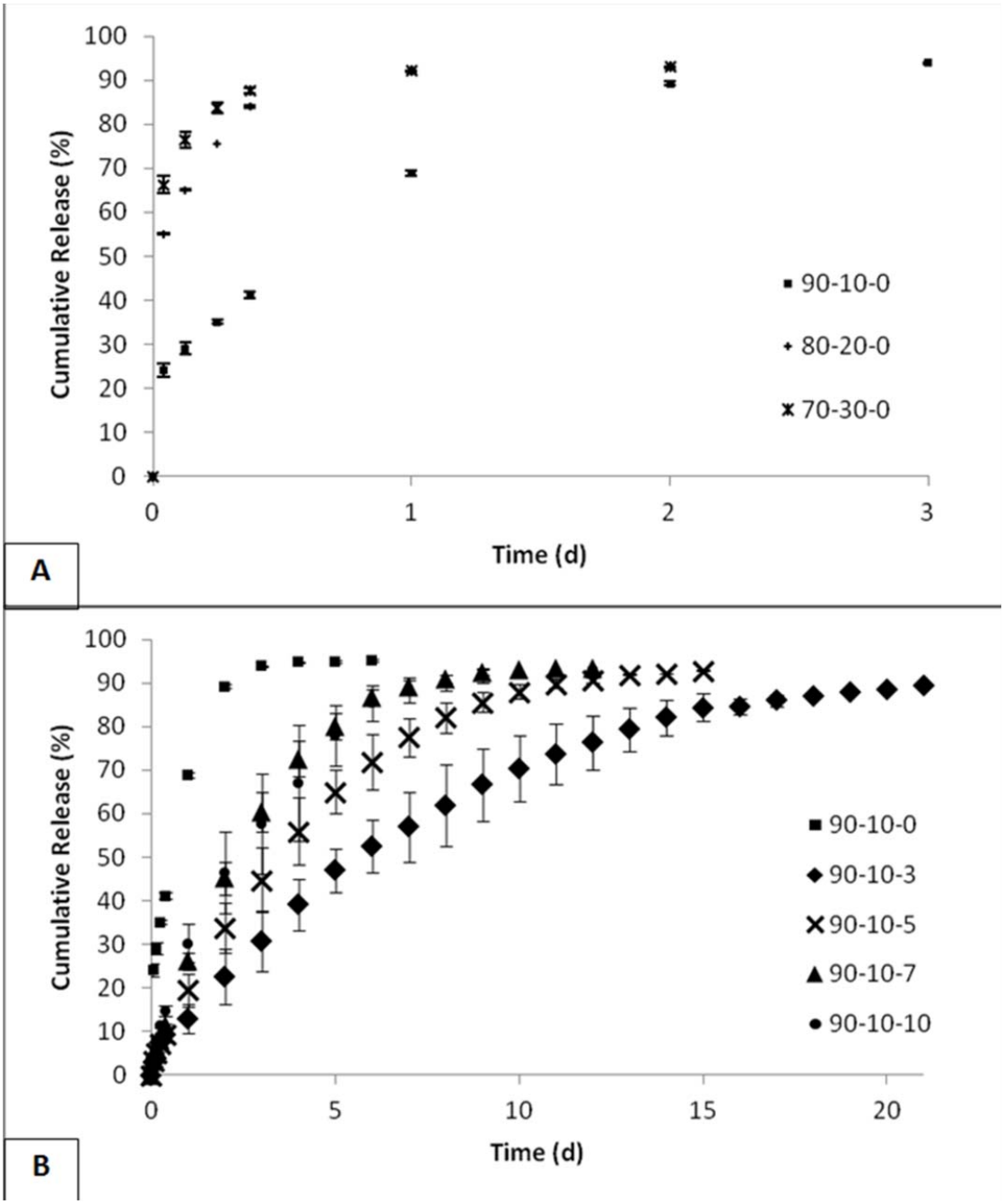

Figure 3: Cumulative NPS release of the scaffolds prepared from different formulations: (A) different PCL to PLLA ratio and (B) different H_2O to HFIP ratio. Faster release of NPS was observed from scaffolds with higher PCL to PLLA ratio. The addition of 3 vol% H_2O has resulted in scaffolds that allowed slower release as long as two weeks, though subsequent releases were faster with further increase of H_2O content. (Error bars indicate standard deviation, n = 3).

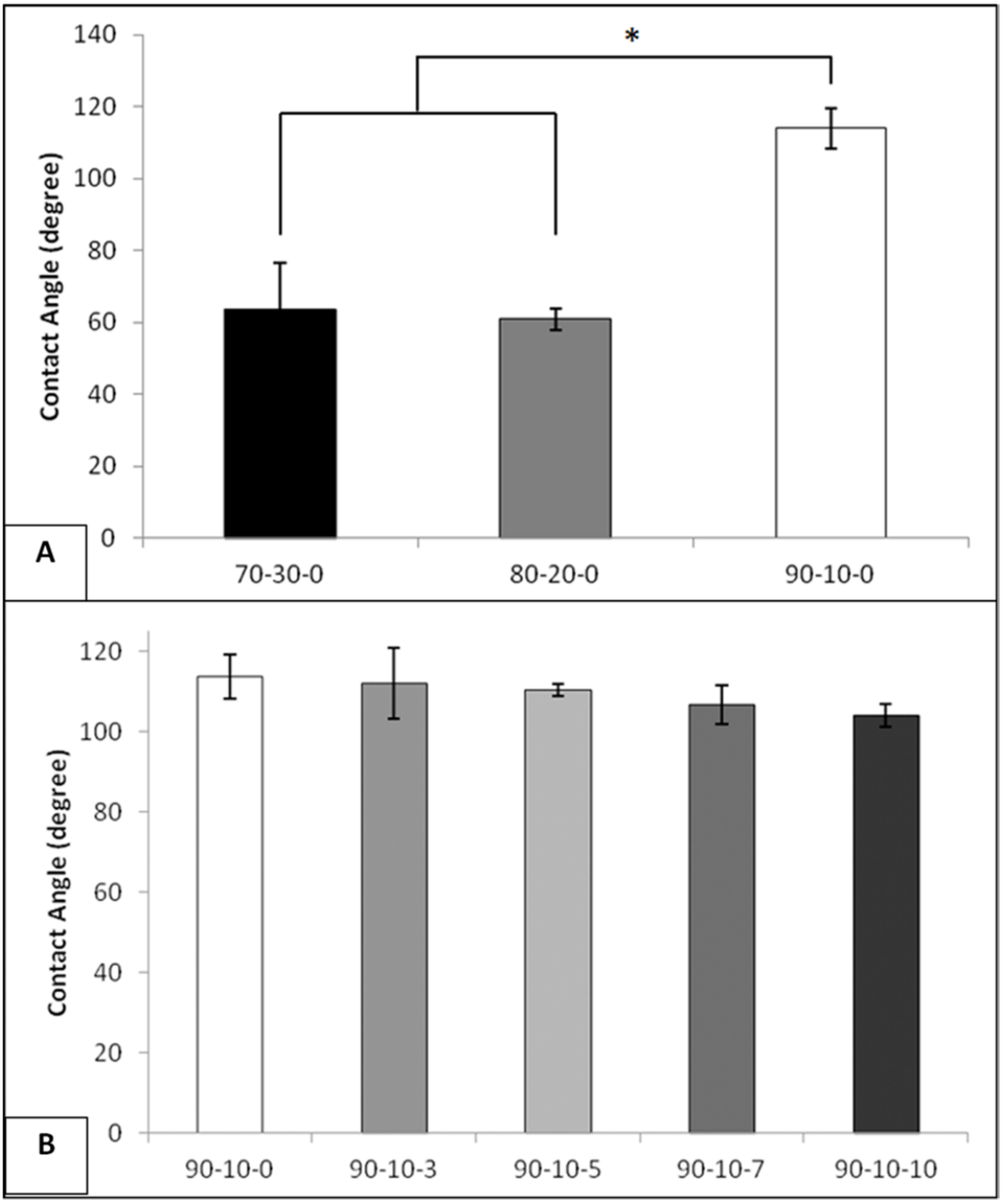

Figure 4: The contact angle of various scaffolds with different (A) PCL to PLLA ratio and (B) H_2O to HFIP ratio. When the PLLA to PCL ratio increased, 90-10-0 has a significant higher contact angle than that of the 70-30-0 and 80-20-0 scaffolds. Meanwhile for variation of the percentage of H_2O as the co-solvent, the contact angle of the scaffolds did not change significantly. (* indicates $p < 0.05$) (Error bars indicate standard deviation, n = 3).

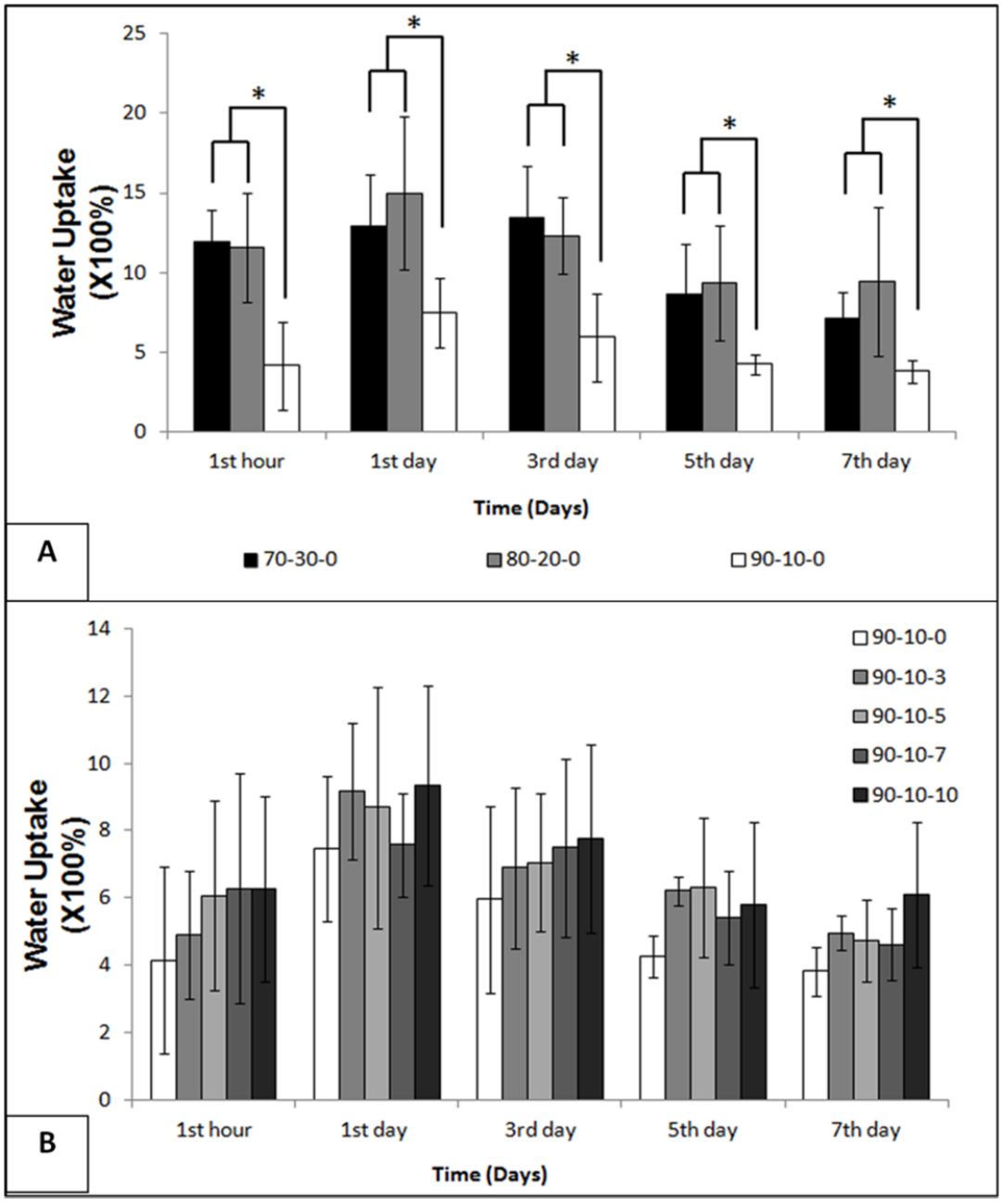

583

584 **Figure 5:** The water uptake of various scaffolds after 7 days of immersion in PBS with different (A) PCL
585 to PLLA ratio and (B) H_2O to HFIP ratio. When the PCL to PLLA ratio increased, 70-30-0 and 80-20-0
586 scaffolds have a significant higher water uptake than that of the 90-10-0. Meanwhile for variation of the
587 percentage of H_2O as the co-solvent, the water uptake of the scaffolds did not change significantly. (*
588 indicates $p < 0.05$) (Error bars indicate standard deviation, $n = 3$).

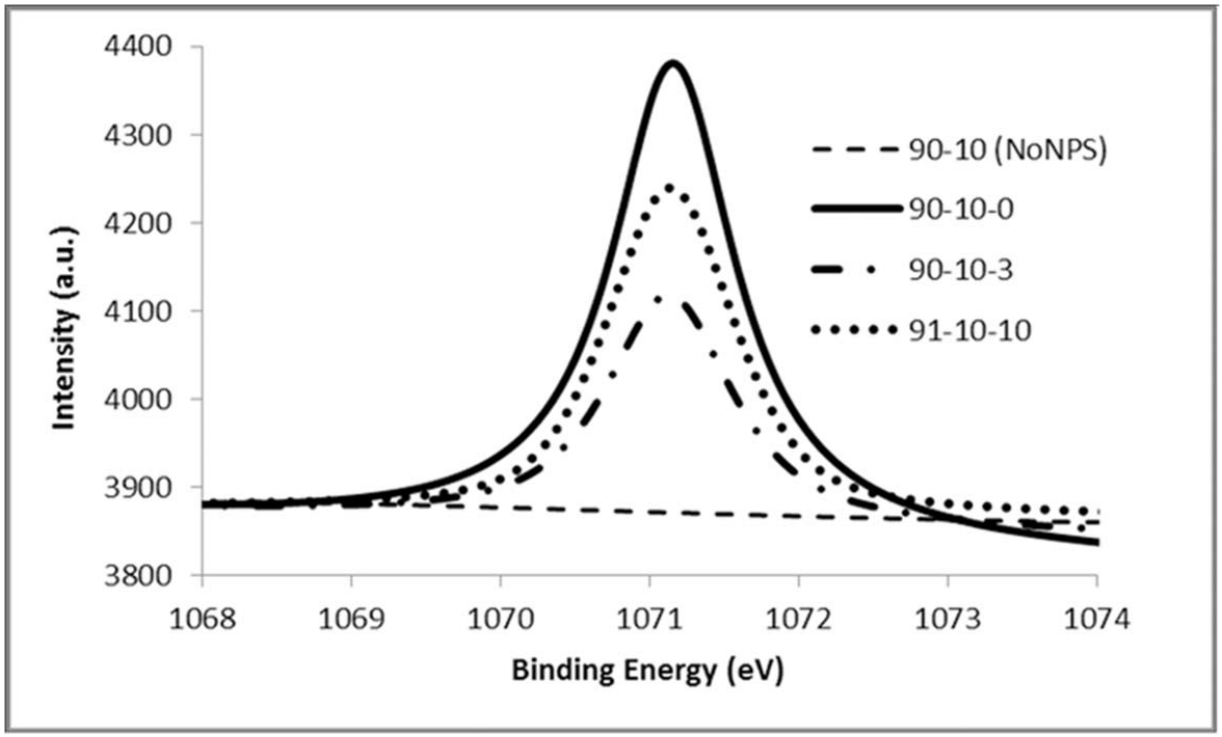

589

590 **Figure 6:** The XPS analysis of the scaffolds with and without NPS. The presence of NPS on scaffold 90-
591 10-0 (solid line), 90-10-3 (dash-dot line) and 90-10-10 (dotted line) was indicated by the sodium
592 characteristic peak (Na 4s), which was at the binding energy of around 1071 eV, while scaffold without
593 NPS (dash line) showed no peak at that particular region. (n = 3).

594

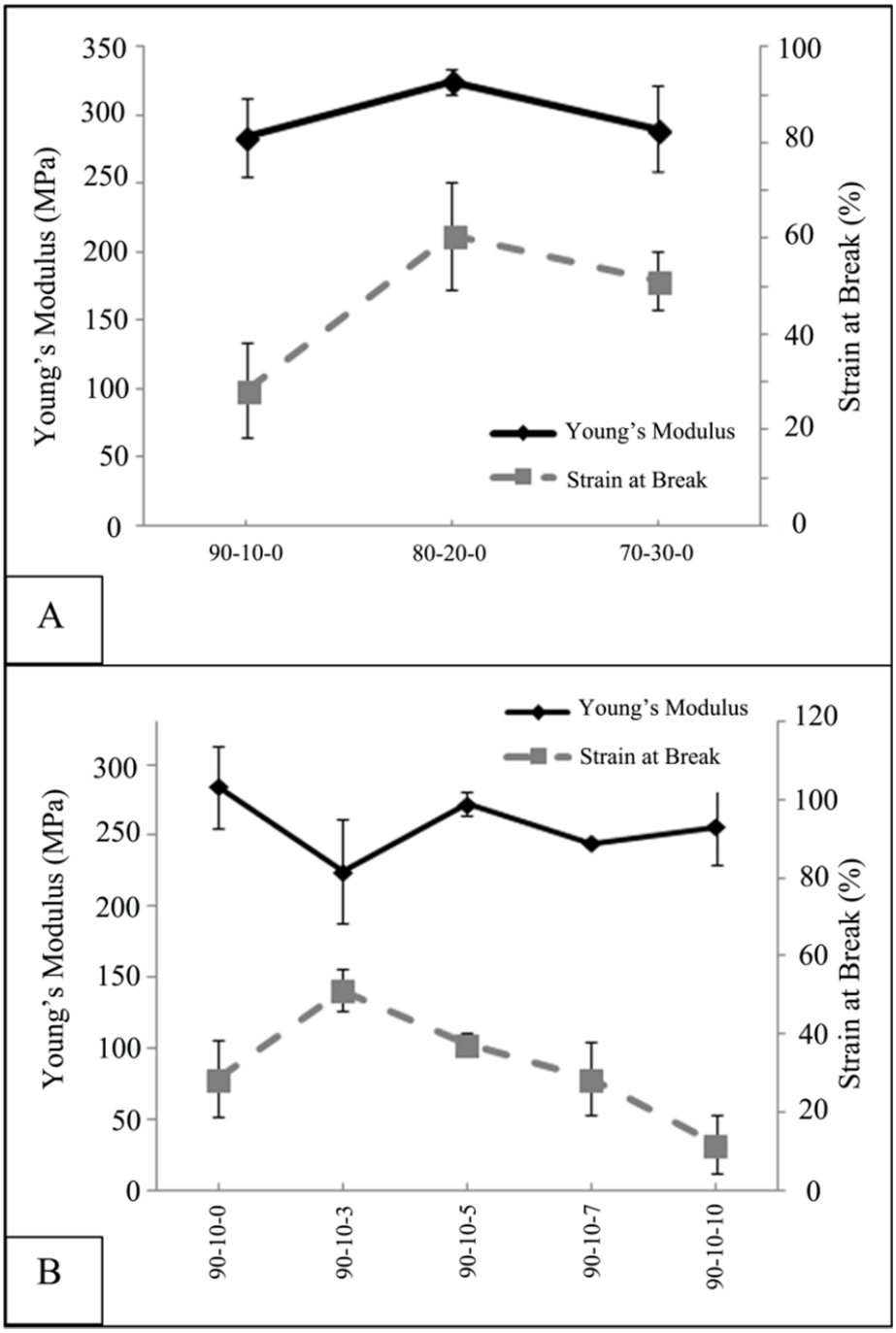

595

596 **Figure 7:** The mechanical properties of the scaffolds prepared from different formulations: (A) different
597 PCL to PLLA ratio and (B) different H_2O to HFIP ratio. There was no significant difference in Young's
598 modulus for all formulations. Higher PCL to PLLA ratio has resulted in scaffolds with higher elasticity.
599 With minimal amount of H_2O (3 vol%), elasticity of the scaffolds increased though elasticity dropped
600 with increasing H_2O content. (Error bars indicate standard deviation, n = 3).

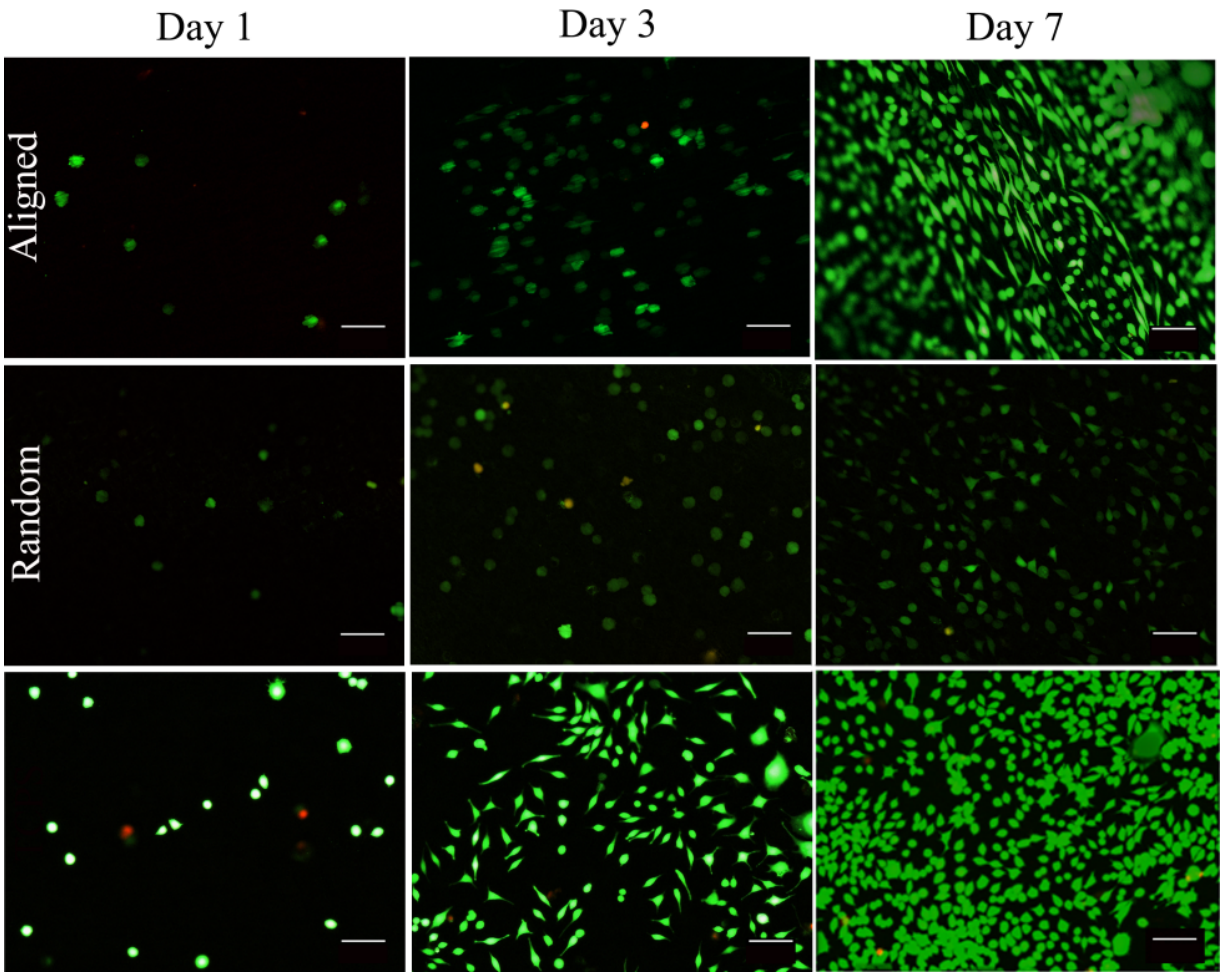

Figure 8: Fluorescence microscopy images of L929 cultured samples over 7 days. Viable cells (green) were stained by calcein-AM while nuclei of non-viable cells (red) were stained by ethidium homodimer-1. Cells on the aligned scaffold started to spread from day3, proliferated and arranged themselves according to the fibers alignment by day7. (n = 3). (Scale bar = 10μm).

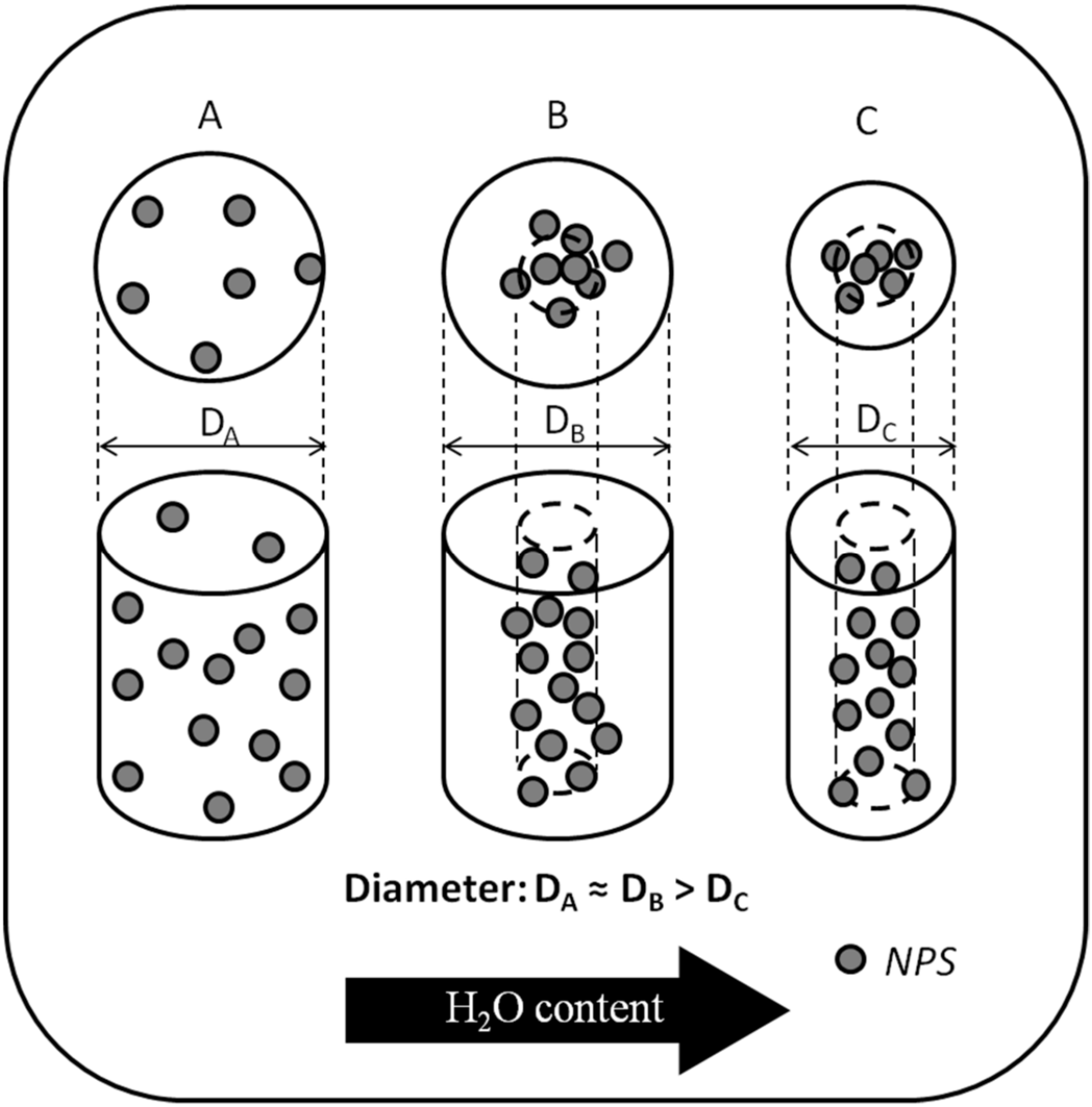

607

608 **Figure 9:** Schematic showing the possible NPS distribution within the fibers when the H_2O content
609 increased as the co-solvent in electrospinning solutions: (A) NPS was evenly distributed inside the fibers
610 when no water was added; (B) more NPS tend to stay inside the fibers with the presence of minimal
611 amount of H_2O; however, (C) further increase the amount of H_2O yielded thinner fibers and more NPS on
612 the surface of the fibers.

613

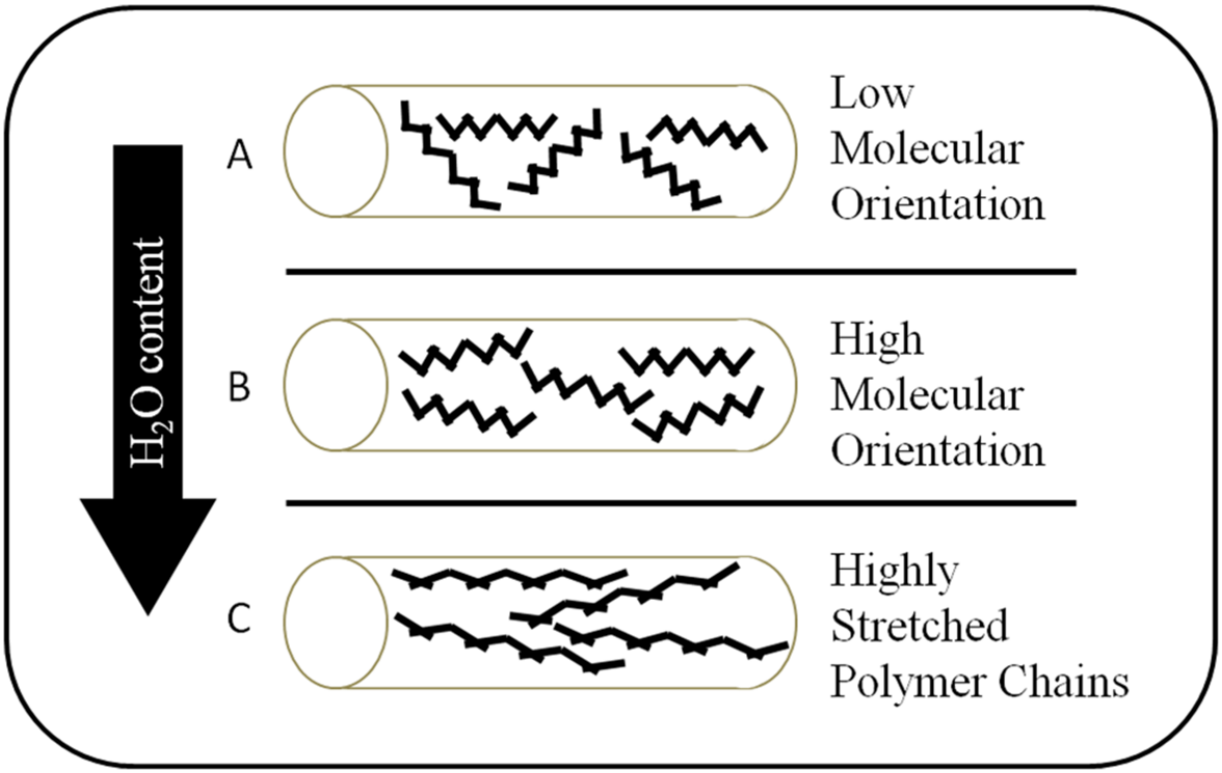

614

615 **Figure 10:** Schematic showing the possible molecular changes when the H_2O content increased as the co-
616 solvent in electrospinning solutions: (A) polymer chains have lower molecular orientation when no water
617 was added; (B) polymer chains have higher molecular orientation with the presence of small amount of
618 H_2O; (C) polymer chains were highly stretched with further addition of H_2O.

Tables

Table 1: Description of different formulations of electrospinning solutions

Samples	PLLA (wt%)	PCL (wt%)	NPS (wt%)	HFIP (vol%)	H_2O (vol%)
70-30-0	5.6%	2.4%	0.4%	100%	0%
80-20-0	6.4%	1.6%	0.4%	100%	0%
90-10-0	7.2%	0.8%	0.4%	100%	0%
90-10-3	7.2%	0.8%	0.4%	97%	3%
90-10-5	7.2%	0.8%	0.4%	95%	5%
90-10-7	7.2%	0.8%	0.4%	93%	7%
90-10-10	7.2%	0.8%	0.4%	90%	10%

Table 2: Summary of the characterization results of scaffolds produced from different formulations of electrospinning solutions.

Samples	Mean Fiber Diameter (µm)	Young's Modulus (Mpa)	Tensile Strength (Mpa)	Strain at Break (%)
70-30-0	0.944 ± 0.096	290.31 ± 31.36	24.99 ± 1.13	51.33 ± 6.06
80-20-0	1.090 ± 0.233	325.03 ± 9.38	27.18 ± 0.39	60.69 ± 11.25
90-10-0	1.071 ± 0.153	284.18 ± 28.58	20.04 ± 1.80	28.44 ± 9.87
90-10-3	0.995 ± 0.221	224.41 ± 36.44	14.99 ± 2.70	51.29 ± 5.56
90-10-5	0.954 ± 0.197	272.15 ± 8.38	18.87 ± 0.37	37.29 ± 3.03
90-10-7	0.836 ± 0.171	244.37 ± 1.78	16.76 ± 1.01	28.51 ± 9.27
90-10-10	0.760 ± 0.176	256.26 ± 26.77	14.57 ± 1.23	11.72 ± 7.34